Functional inhibition of Oct leads to HNF4α upregulation

JOHANNA VOLLMAR[1], YONG OOK KIM[2], JENS UWE MARQUARDT[3], PETER R. GALLE[4], DETLEF SCHUPPAN[2] and TIM ZIMMERMANN[1]

[1]Department of Internal Medicine II, Hospital of Worms, D-67550 Worms; [2]Institute of Translational Immunology, Fibrosis and Metabolism Centre, Johannes Gutenberg-University Mainz, D-55131 Mainz; [3]Department of Internal Medicine I, University Hospital Schleswig-Holstein, D-23538 Lübeck; [4]1st Department of Internal Medicine, Gastroenterology and Hepatology, University Medical Centre, Johannes Gutenberg-University Mainz, D-55131 Mainz, Germany

Received May 11, 2020; Accepted December 21, 2020

DOI: 10.3892/etm.2021.9780

Abstract. Organic cation transporters (human, OCT; mouse, Oct) are responsible for the intracellular uptake and detoxification of a broad spectrum of endogenous and exogenous substrates. The OCT1 gene SLC22A1 (human; mouse, Scl22a1) is transactivated by hepatocyte nuclear factor 4α (human, HNF4α; mouse, Hnf4α). HNF4α is a master regulator of hepatocyte differentiation and is frequently associated with hepatocellular carcinoma (HCC). In addition, the downregulation of HNF4α is associated with enhanced fibrogenesis. Our recent study revealed that hepatocarcinogenesis and fibrosis were enhanced with the loss of Oct3 (gene, Slc22a3). Notably, differences in Hnf4α expression, and in cholestasis and fibrosis were also detected in Oct3-knockout (FVB. Slc22a3tm10pb, Oct3$^{-/-}$) mice. To the best of our knowledge, no data exists on an interaction between Oct3 and Hnf4α. We hypothesised that loss of Oct3 may have an impact on Hnf4α expression. In the present study, gene expression analyses were performed in liver tissue from untreated Oct3$^{-/-}$ and wild type (FVB, WT) mice. C57BL/6, Oct3$^{-/-}$ and WT mice were treated with pro-fibrotic carbon tetrachloride (CCl_4) or thioacetamide (TAA) for 6 weeks to chemically induce liver fibrosis. Cholestasis-associated fibrosis was mechanically generated in Oct3$^{-/-}$ and WT mice by bile duct ligation (BDL). Finally, stably OCT1- and OCT3-transfected tumour cell lines and primary murine hepatocytes were treated with the non-selective OCT inhibitor quinine and Hnf4α expression was quantified by qPCR and immunofluorescence. The results revealed that Hnf4α is one of the top upstream regulators in Oct3$^{-/-}$ mice. Hnf4α mRNA expression levels were downregulated in Oct3$^{-/-}$ mice compared with in WT mice during cholestatic liver damage as well as fibrogenesis. The downregulation of Hnf4α mRNA expression in fibrotic liver tissue was reversible within 4 weeks. In stably OCT1- and OCT3-transfected HepG2 and HuH7 cells, and primary murine hepatocytes, functional inhibition of OCT led to the upregulation of Hnf4α mRNA expression. Hnf4α was revealed to be located in the cytosol of WT hepatocytes, whereas Oct3$^{-/-}$ hepatocytes exhibited nuclear Hnf4α expression. In conclusion, Hnf4α was downregulated in response to cholestasis and fibrosis, and functional inhibition of Oct may lead to the upregulation of Hnf4α.

Correspondence to: Dr Johanna Vollmar, Department of Internal Medicine II, Hospital of Worms, Gabriel-von-Seidl-Street 81, D-67550 Worms, Germany
E-mail: johannilein@yahoo.de

Abbreviations: Oct1/2/3, organic cation transporter 1/2/3; Oct3$^{-/-}$, Oct3-knockout; WT, wild-type; CCl_4, carbon tetrachloride; TAA, thioacetamide; RT-qPCR, reverse transcription-quantitative polymerase chain reaction; HNF4α, hepatocyte nuclear factor 4α; BDL, bile duct ligation

Key words: organic cation transporter, HNF4α, SLC22A1, SLC22A3

Introduction

Organic cation transporters (human: OCT, mouse: Oct) are membrane transport proteins involved in many metabolic processes. Recently, we and others found that downregulation of OCT1 is associated with tumour progression in human hepatocellular and cholangiocellular carcinoma (1-4). Furthermore, we demonstrated that the loss of Oct3 (gene: Scl22a3) leads to enhanced proliferation and hepatocarcinogenesis (5).

OCT expression is regulated via complex mechanisms. The OCT1 gene SCL22A1 (mouse: Scl22a1) is trans activated by hepatocyte nuclear factor 4alpha (human: HNF4α, mouse: Hnf4α) (6). Glucocorticoid receptor induced expression of HNF4α was found to contribute to indirect OCT1 gene upregulation in primary human hepatocytes, but not in hepatocyte-derived tumour cell lines (7).

HNF4α is a master regulator of hepatocyte differentiation and metabolism, controlling the development of the hepatic epithelium, liver morphogenesis (8) and hepatic metabolic function (9). This nuclear factor is also known as a tumour suppressor (10). For example, HNF4α deletion promotes diethyl nitrosamine-induced hepatocellular carcinoma in mice (11) and HNF4α inhibition blocks hepatocyte differentiation and promotes biliary cancer (12). Furthermore, overexpression of HNF4α in human mesenchymal stem cells suppresses hepatocellular carcinoma development through downregulation of

the Wnt/β-catenin signalling pathway (13). HNF4α also seems to play a pivotal role in fibrosis progression, as the downregulation of HNF4α aggravates hepatic fibrosis in rats (14). Vice versa, Fan *et al* described a regression effect of HNF4α on liver cirrhosis in rats (15) and HNF4α-induced hepatic stem cells ameliorated chronic liver injury in liver fibrosis models (16).

Oct3 deficient mice (FVB.Slc22a3tm1Dpb, Oct3$^{-/-}$) do not have an obvious phenotype (17). but we have recently shown enhanced proliferation, hepatocarcinogenesis and fibrosis progression in these mice (5,18). We studied Oct3$^{-/-}$ mice in different models of liver damage (DEN/Phenobarbital, bile duct ligation (BDL), carbon tetrachloride (CCl_4) treatment) in order to analyse Oct1 regulation. The knockout mice showed a hepatic phenotype with enhanced Ki-67 staining, leucocyte infiltration and fibrosis quantified by hydroxyproline assay and Sirius red staining (5,18). Hence, the upstream regulatory mechanism is still unclear. Surprisingly, we also found differences in Hnf4α expression in cholestasis and fibrosis in Oct3$^{-/-}$ mice. Oct1 and Oct3 are both expressed in the liver (19) and substitute each other (17,20). To date no data exists on an interaction between Oct3 and Hnf4α. We hypothesised that loss of Oct3 has an impact on Hnf4 α expression. Therefore, we analysed Hnf4α expression in different fibrosis models in Oct3$^{-/-}$ and wild type (FVB, WT) mice, stably transfected tumour cell lines and primary murine hepatocytes.

Materials and methods

Animals. Animal care (housing, husbandry conditions) and animal procedures were performed in accordance with the European Council Directive of 24 November, 1986 (86/609/EEC), and the present study was approved by the state animal care commission (Koblenz; approval number, 23 177-07/G 14-1-010). Mice received standard food for rodents (Altromin Lage, Nr. 1314) with free access to food and water. They were kept in groups of five siblings of the same sex per cage with constant temperatures of 22-24˚C and humidity of 55±10% as well as a 12-h day and night rhythm. Male Oct3-knockout (FVB.Slc22a3tm1Dpb, Oct3$^{-/-}$) (17), their WT littermates (FVB) and C57BL/6 mice (in total n=51), 4-6 weeks old with an average body weight of 20 g at the start of the experiment, were used in this study. Oct3$^{-/-}$ mice were kindly provided by Prof. Schinkel, Cancer Centre Amsterdam. C57BL/6 and WT mice were bred by the Translational Animal Research Centre (TARC) of the University Medical Centre, Johannes Gutenberg-University Mainz. To investigate the relevance of Oct3 expression and the effects on cholestasis and fibrosis, two different animal models of fibrosis were analysed: i) Chemically induced liver fibrosis by the application of pro-fibrotic carbon tetrachloride (CCl_4) or thioacetamide (TAA) for 6 weeks; and ii) cholestasis-associated fibrosis after 7 days of bile duct ligation (BDL).

Gene expression analysis. Total RNA was extracted from livers of three 5-week-old untreated WT and Oct3$^{-/-}$ mice using the High Pure RNA tissue kit (cat. no./ID: 11828665001; Roche Diagnostics) following the manufacturer's instructions. RNA quantity and purity were estimated using a NanoDrop ND-1000 Spectrophotometer (NanoDrop Technologies) and integrity was assessed by Agilent 2100 Bioanalyzer (Agilent Technologies). cDNA libraries were generated using the QuantSeq 3'mRNA-Seq Library Prep kit for Illumina (Lexogen, Vienna, Austria) following the manufacturer's instructions (21). RNA sequencing was performed using Illumina HiSeq Rapid Mode by the Institute of Human Genetics, Department of Genomics, Life & Brain Center, University of Bonn. The sequencing kit was HiSeq 3000/4000 SBS Kit (single read, 50 cycles) (cat. no./ID: FC-410-1001; Illumina). Coverage was standard 3' Seq. The loading concentration of DNA was 0.06-0.44 nmol assuming a nucleotide length of 100-300 bp. Data were deposited at the BioProject database (http://www.ncbi.nlm.nih.gov/bioproject/685115, BioProject ID PRJNA685115). The read sequences were aligned to the Mus_musculus.GRCm38.74 reference genome followed by read mapping and read counting, as described before using the Bioconductor package Rsubread (V 1.24.2) (22). Before aligning reads, low quality reads were filtered, reads containing adapter sequences, and duplicate mapping reads using Bioconductor package ShortRead (V 1.32.1) (23). For differential expression analysis (WALD-Test) the Bioconductor package DESeq2 (V 1.14.1) with an adjusted P-value <0.01 was used (24). All data analysis was performed using R programming language and related packages.

Functional classification and network analysis were performed using Ingenuity Pathway Analysis (Ingenuity Systems Inc.). The significance of each network, function and pathway was determined by the scoring system provided by Ingenuity Pathway Analysis tool. Data will be provided on demand.

Induction of fibrosis. C57BL/6, WT and Oct3$^{-/-}$ mice, 4-6 weeks old, were treated with pro-fibrotic thioacetamide (TAA) or CCl_4 for 6 weeks (25). TAA was injected intraperitoneally three times a week in escalating doses, starting with 50 mg/kg (doses 1 and 2, week 1), 100 mg/kg (doses 2 to 5, weeks 1-2), 200 mg/kg (doses 6 to 10, weeks 2-4), 300 mg/kg (doses 11 to 15, weeks 4-5), and 400 mg/kg (dose 16 onwards, week 6). Placebo intraperitoneal injection served as the control. CCl_4 was administered three times a week by oral gavage in escalating doses 50/50 vol/vol mixed with mineral oil: 0.875 ml/kg (dose 1 dose, week 1), 1.75 ml/kg (doses 2 to 7, weeks 1-2), 2.5 ml/kg (doses 8 to 13, weeks 3-4), and 3.25 ml/kg (after week 4). Oral gavage of mineral oil served as the control. Animals were culled by cervical dislocation after 6 weeks of treatment or after 1 to 4 weeks of reversal, death was confirmed by loss of heartbeat through direct cardiac palpation and tissues were harvested for qPCR and histological analysis.

Induction of cholestasis. WT and Oct3$^{-/-}$ mice, 7-10 weeks old (body weight 18-20 g), underwent bile duct ligation (BDL) or placebo surgery (sham operation) as previously described under anaesthesia with 100 mg/kg Ketamine and 20 mg/kg Rompun (i.p) (26-28). Animals were sacrificed by cervical dislocation after 7 days; death was confirmed by loss of heartbeat and tissues were harvested for qPCR and histological analysis.

RNA isolation and RT-qPCR analysis. Total RNA was extracted from liver tissue using the High Pure RNA Tissue Kit (Roche Diagnostics) and cDNA synthesis was performed using the iScript cDNA Synthesis kit (Bio-Rad) according to

the manufacturer's recommendations. Quantitative analysis of Oct1 (Slc22A1) transcripts was performed by quantitative real-time reverse transcriptase (RT-) polymerase chain reaction (qPCR). The Quantitect SYBR-Green PCR Kit (Qiagen) and validated primers of a Quantitect Primer Assay with the primer sets Mm_SLC22A1_2_SG (OCT1; 84 bp fragment), Mm_HNF4α (HNF4α; 100 bp fragment forward, 5'-GGATATGGCCGACTACAGCG-3' and reverse, 5'-AGATGGGGACGTGTCATTGC-3') and Mm_GAPDH_3_SG (GAPDH; 144 bp fragment) (Qiagen) were used according to the manufacturer's instructions. For the amplification, an initial denaturation at 95˚C for 15 min, followed by 15 sec at 94˚C, 30 sec at 55˚C and 30 sec at 72˚C for 40 cycles was used. Samples were run on a LightCycler® 480 real-time PCR system (Roche Diagnostics). The relative expression levels were calculated by normalisation to GAPDH gene expression using the LightCycler® 480 software Release 1.5.0.

Western blot analysis. Total protein extracts were prepared in sample buffer pH 8.0 containing 20 mM Tris, 5 mM EDTA, 0.5% Triton X-100 and EDTA-free protease inhibitors (Complete Mini, 1:25; Roche Diagnostics). For western blot analysis 60 μg total protein was separated by a 12% SDS-PAGE gel. The gel was transferred onto a nitrocellulose transfer membrane (OPTITRAN BA-S85/Whatman) following separation. Rabbit anti-HNF4α monoclonal antibody (1:1,000; Abcam) or goat anti-actin polyclonal antiserum (1:1,000; Santa Cruz Biotechnology, Inc.) were used as the primary antibodies. Horseradish peroxidase (HRP)-conjugated anti-rabbit or anti-goat IgG (Santa Cruz Biotechnology, Inc.) was used as the secondary antibody at a 1:10,000 dilution. Protein bands were visualised using Western Lightning® Plus-ECL enhanced chemiluminescent substrate (Perkin Elmer).

Immunofluorescence. Primary murine hepatocytes were incubated with rabbit-polyclonal-anti Hnf4α (Bioss Antibodies Inc.) as the primary antibody after preincubation with hydrogen peroxide for blocking of endogenous peroxidase. Endogenous biotin was blocked with the Avidin-Biotin Blocking kit (Vector Laboratories) and contaminating proteins were inhibited by ROTI®-Immunoblock solution (ROTH). After incubation with the secondary antibody (goat anti-rabbit IgG-Biotin, 1:1,000; Dako Cytomation), the TSA™ Cyanine system (Perkin Elmer) was added. For the negative control, the primary antibody was omitted. The images were evaluated under a fluorescence microscope (Olympus BX51, Olympus U-RFL-T).

Oct inhibition. HepG2 (ATCC® HB-8065™), a human liver cancer cell line, and HuH7 (RRID: CVCL_0336), a well differentiated hepatocyte-derived carcinoma cell line, were grown at 37˚C in a humidified atmosphere (5% CO_2) in plastic culture flasks (Falcon 3112; Becton-Dickinson). The medium was Dulbecco's modified Eagle's medium (31885-023; Life Technologies) supplemented with 10% foetal calf serum (Life Technologies). Medium was changed every 2-3 days and the culture was split every 7 days.

The pcDNAOCT1 and pcDNAOCT3 plasmids and an empty vector (Invitrogen; Thermo Fisher Scientific, Inc.) were stably transfected into HepG2 and HuH7 cells by mixing with the Attractene Transfection Reagent (Qiagen) according to the instructions of the manufacturer. Primary hepatocytes were isolated from $Oct3^{-/-}$ and WT mice and cultured in collagen-coated 24-well culture plates ($2.5x10^5$/ml) as previously described (29). For functional inhibition of the transporters, primary murine hepatocytes were treated with different doses (0, 50, 100 and 150 μM) of the standard non-selective OCT inhibitor quinine (Sigma-Aldrich; Merck KGaA) for 48 h (30-35).

Statistical analysis. Data management and statistical analysis were performed with Prism version 7.0 (GraphPad Software, Inc.). Results are expressed as means ± SEM and represent data from a minimum of three independent experiments assessed in triplicates. Three biological replicates were assumed being the minimum for any inferential analysis (biological repetition). As sample numbers were small, normal distribution was assumed. Therefore, no normality test was necessary. When two groups were compared, unpaired Student's t-test was used. Data with more than two groups were analysed by one-way or two-way ANOVA with Dunnett's multiple comparisons test after one-way ANOVA and Tukey-Kramer test after two-way ANOVA. For Pearson's correlation analysis SPSS program (version 23.0; IBM Corp.) was used. $P<0.05$ was considered statistically significant.

Results

Hnf4α is one of the top upstream regulators in $Oct3^{-/-}$ mice. Transcriptome analysis showed that Hnf4α is one of the top upstream regulators in $Oct3^{-/-}$ mice ($P<0.001$), with 110 target molecules. Hnf4α plays a pivotal role in regulating various transmembrane proteins and enzymes in $Oct3^{-/-}$ mice (Fig. 1A). The majority of genes regulated by Hnf4α were upregulated in $Oct3^{-/-}$ mice (Fig. 1B). Other significantly upregulated (positive z-score) upstream regulators were the (proto-) oncogenes myc ($P=1.59x10^{-13}$; $z=2.21$) and kras ($P=5.43x10^{-7}$; $z=0.77$), while the tumour suppressor tp53 was significantly downregulated (negative z-score) in $Oct3^{-/-}$ mice ($P=1.1x10^{-7}$; $z=-3.15$) (Fig. 1C).

Deletion of Oct3 leads to Hnf4α mRNA downregulation in cholestasis and fibrosis. Untreated $Oct3^{-/-}$ mice did not show differences in Hnf4α mRNA expression in comparison to WT littermates at the age of 4 weeks (Fig. 2A). Hnf4α mRNA expression was significantly downregulated in cholestatic $Oct3^{-/-}$ mice (n=6) in comparison to WT mice (n=8) 7 days after BDL ($P<0.01$) (Fig. 2B).

Also, after chemical fibrosis induction with 6 weeks of CCl_4 treatment, Hnf4α mRNA expression was significantly downregulated in $Oct3^{-/-}$ mice (n=7) as compared to WT mice (n=9) ($P<0.001$) (Fig. 2C).

Hnf4α mRNA downregulation in fibrosis is reversible. Fibrosis was induced with TAA and CCl_4 treatment for 6 weeks in C57BL/6 mice (n=5), which are susceptible to conventional toxin-induced fibrosis progression and reversal models. Hnf4α mRNA expression was quantified by qPCR at the end of the treatment period and after up to four weeks of reversal. After 6 weeks of TAA and CCl_4 treatment, Hnf4α mRNA expression was significantly downregulated in fibrotic mouse livers

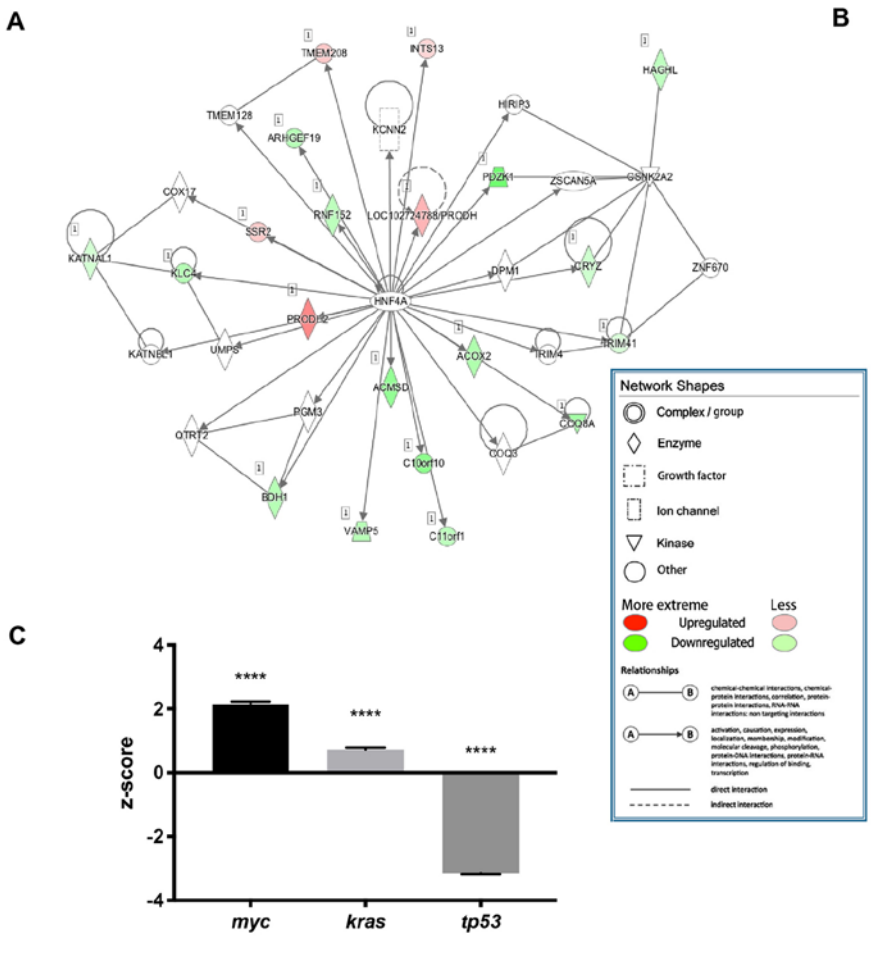

Genes	Prediction	Expr Log Ratio
CYP3A5	Upregulated	2.868
CYP2C8	Upregulated	2.836
Cyp2a12/Cyp2a22	Upregulated	2.501
ASGR2	N.s. regulated	2.130
APOA1	Upregulated	2.118
SERPINA1	Upregulated	2.110
APOA2	Upregulated	2.100
CYP2E1	N.s. regulated	2.053
ABCB11	N.s. regulated	2.005
PRODH2	N.s. regulated	1.890
APOM	Upregulated	1.879
CYP3A7	Upregulated	1.740
ABCB9	N.s. regulated	1.730
ANG	N.s. regulated	1.685
SGK2	N.s. regulated	1.524
TTR	Upregulated	1.454
SLC39A6	N.s. regulated	1.347
F13B	N.s. regulated	1.305
PCNA	Downregulated	1.274
MPZL2	N.s. regulated	1.270
PEMT	N.s. regulated	1.255
POLR1B	N.s. regulated	1.186
LOC102724788/PRODH	Upregulated	1.167
OTC	Upregulated	1.061
MRTO4	N.s. regulated	1.043
CLDN3	N.s. regulated	1.040
DIS3	N.s. regulated	1.040
ARMC6	N.s. regulated	1.035
CLDND1	N.s. regulated	1.024
BRIP1	N.s. regulated	0,978
WDR12	N.s. regulated	0,932
AGPAT1	N.s. regulated	0,910
POP5	N.s. regulated	0,905
RPS25	N.s. regulated	0,901
TMA16	N.s. regulated	0,889
AQP1	Upregulated	0,872
TMEM208	N.s. regulated	0,853
NOC3L	N.s. regulated	0,842
SSR2	N.s. regulated	0,837
SCARB1	Upregulated	0,805
TMEM33	N.s. regulated	0,794
MDH2	N.s. regulated	0,784
CAMK2D	N.s. regulated	0,782
LSR	N.s. regulated	0,742
UTP23	N.s. regulated	0,731
FARSB	N.s. regulated	0,691
YBX1	N.s. regulated	0,686
NOP16	N.s. regulated	0,686
ATF6B	N.s. regulated	0,670
PERP	Upregulated	0,649

Figure 1. Gene expression analysis. (A) Hnf4α network in Oct3$^{-/-}$ (n=3) mice. Network shapes: Double circle, complex/group; diamond, enzyme; square, growth factor; box, ion channel; triangle, kinase; circle, other; green, upregulated genes; red, downregulated genes; line, direct interaction; dashed line, indirect interaction; arrow, causation. (B) Hnf4α dependent genes in Oct3$^{-/-}$ (n=3) mice. The majority of Hnf4α dependent genes in Oct3$^{-/-}$ mice is upregulated. (C) Activation status (z-score) of the three top upstream regulators in Oct3$^{-/-}$ mice (n=3); while myc and kras are significantly upregulated, tp53 is significantly downregulated in Oct3$^{-/-}$ compared to WT mice. Results were normalized to WT results. ****P<0.0001 vs. WT mice. Hnf4α, hepatocyte nuclear factor 4α; Oct3$^{-/-}$, Oct3-knockout (FVB.Slc22a3tm10pb); N.s., not significant.

(P<0.01 compared to baseline). After reversal for one and four weeks, the Hnf4α mRNA level increased again (Fig. 2D and E). Hnf4α mRNA expression correlated well with Oct1 mRNA expression (Fig. 2F).

Functional inhibition of Oct induces Hnf4α mRNA expression. Oct regulation cannot be easily studied, as the transporters are not relevantly expressed in cell lines (36). Therefore, experiments with stably OCT1- and OCT3-transfected tumour cell lines (HepG2 and HuH7, n=4) and primary hepatocytes isolated from Oct3$^{-/-}$ (n=6) and WT (n=4) mice were performed. Proof that transfection with pcDNAOCT1 and pcDNAOCT3 induced overexpression of OCT1 and OCT3 compared with the empty vector was provided as Fig. S1. Hnf4α mRNA expression was significantly upregulated in OCT1- and OCT3-transfected HepG2 and HuH7 cells compared with in tumour cells transfected with empty vector (Fig. 3A) and primary Oct3$^{-/-}$ hepatocytes (Fig. 3B) after treatment with the Oct inhibitor quinine (P<0.01). Western blots and immunofluorescence in primary WT and Oct3$^{-/-}$ hepatocytes showed an increase of Hnfα protein expression with escalating quinine doses (Figs. 3C and S2-4). These data clearly show that functional loss of Oct induces the expression of Hnf4α. Interestingly, immunofluorescence of primary murine hepatocytes showed that Hnf4α was not only increased with escalating quinine doses, but theHnf4α distribution also differed between Oct3$^{-/-}$ and WT hepatocytes. While Hnf4α was located in the cytosol of WT hepatocytes, Oct3$^{-/-}$ hepatocytes showed nuclear Hnf4α expression, indicating that Oct3 affects Hnf4α *in vivo* (Figs. 3C and S5).

Discussion

HNF4α has been extensively studied in many tissues and tumour cell lines, but few data exist about an interaction with OCTs. According to previous findings, Hnf4α is downregulated in fibrosis (14). Chemically induced fibrogenesis with two different agents (CCl_4 and TAA) resulted in Hnf4α mRNA downregulation. Interestingly, the mRNA of this nuclear factor was re-expressed after stopping administration of TAA and CCl_4 when fibrosis reversal occurred, indicating that the Hnf4α downregulation in fibrotic tissue is reversible (Fig. 2A and B). This means that the effect is real, reproducible and relevant. To date, no data exist on the reversibility

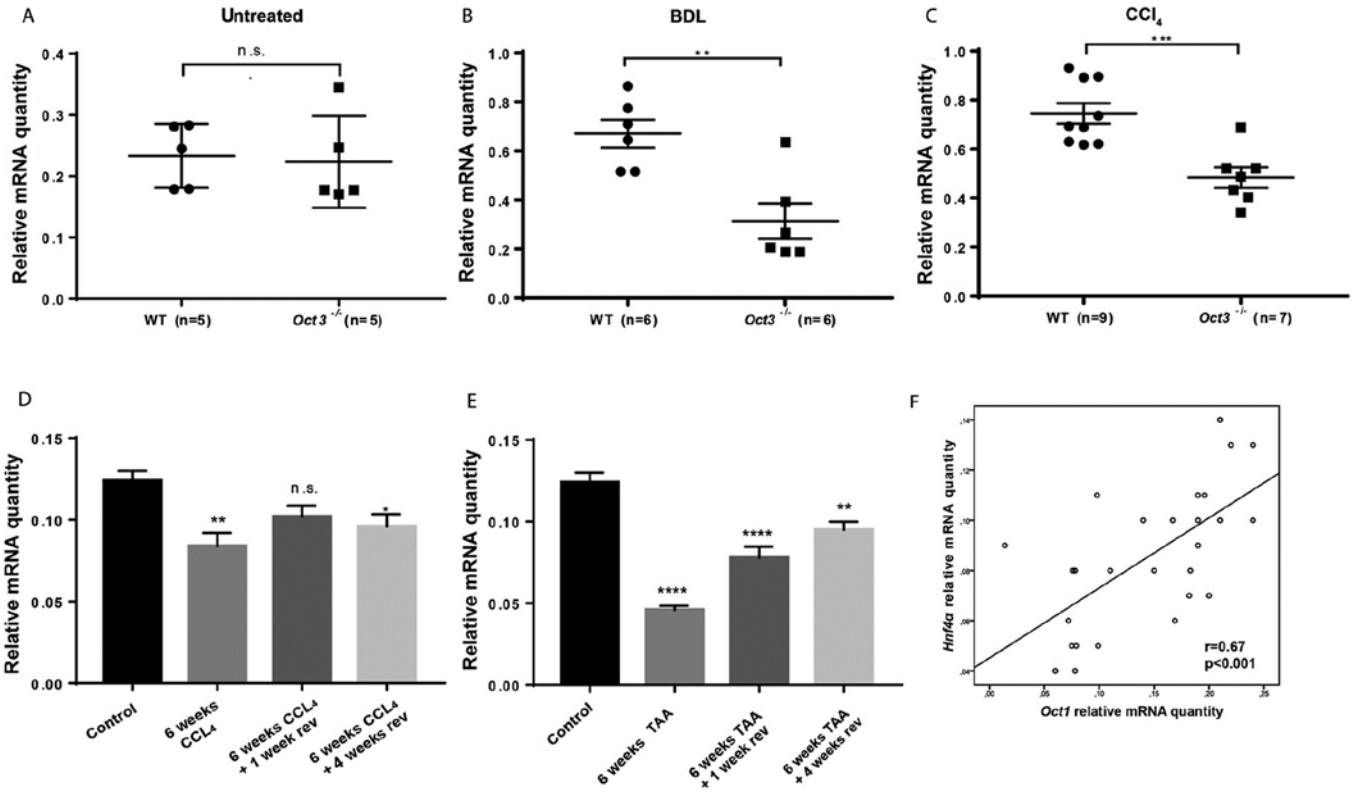

Figure 2. Hnf4α downregulation in cholestasis and fibrosis. (A) Hnf4α mRNA expression in 4 weeks old untreated Oct3$^{-/-}$ (n=5) and WT mice (n=5); no significant difference was detected. (B) Hnf4α mRNA expression in Oct3$^{-/-}$ (n=6) and WT mice (n=6) 7 days after BDL; Hnf4α mRNA expression was significantly downregulated in Oct3$^{-/-}$ mice. Sham operation served as control. Values are expressed as fold expression relative to the control. (C) Hnf4α mRNA expression in Oct3$^{-/-}$ (n=7) and WT mice (n=9) after 6 weeks of CCl_4 treatment: Hnf4α mRNA expression was significantly downregulated in Oct3$^{-/-}$ mice. Oral gavage of mineral oil served as the control. Values are expressed as fold expression relative to the control. (D) Results of Hnf4α mRNA expression after induction of fibrosis with TAA for 6 weeks and after reversal for one and four weeks in C57BL/6 mice (n=5). Placebo intraperitoneal injection and oral gavage of mineral oil served as the control. (E) Results of Hnf4α mRNA expression after induction of fibrosis with CCl_4 for 6 weeks and after reversal for one and four weeks in C57BL/6 mice (n=5). Placebo intraperitoneal injection and oral gavage of mineral oil served as the control. (F) Correlation of Hnf4α and Oct1 mRNA expression after induction of fibrosis with TAA and CCl_4 for 6 weeks and after reversal for one and four weeks in C57BL/6 mice (n=5). *P<0.05, **P<0.01; ***P<0.001; ****P<0.00001 vs. Control. Hnf4α, hepatocyte nuclear factor 4α; Oct3$^{-/-}$, Oct3-knockout (FVB.Slc22a3tm10pb); WT, wild type; TAA, thioacetamide; CCl_4, carbon tetrachloride; BDL, bile duct ligation; n.s., not significant; w, weeks; rev, reversal.

of Hnf4α downregulation in fibrosis, emphasising that confounders do not falsify previous findings. Moreover, the activation of the (proto-) oncogenes myc and kras and the inhibition of the tumour suppressor tp53 in Oct3$^{-/-}$ mice (Fig. 1D) are in line with previous findings of enhanced proliferation and hepatocarcinogenesis with the loss of Oct3 (5). However, the upstream regulatory mechanism is still unclear.

To date, no data exist on a link between OCT3 and HNF4α. The OCT1 gene is transactivated by HNF4α (6), and chemosensitivity to oxaliplatin and 5-FU mediated by OCT1 is induced by HNF4α in renal cell carcinoma (37). Therefore, differences in Hnf4α expression between Oct3$^{-/-}$ and WT mice are likely. There was no difference in Hnf4α mRNA expression between untreated Oct3$^{-/-}$ and WT mice (Fig. 2D), but upon induction of fibrosis or cholestasis, the downregulation of Hnf4α mRNA was more intense in Oct3$^{-/-}$ mice (Fig. 2E and F). This clearly shows that Hnf4α regulation is affected in cholestasis and fibrosis in Oct3$^{-/-}$ mice. Because Hnf4α is a master regulator of hepatocyte differentiation (8) and fibrosis progression (14), these findings may contribute to identify Hnf4α as an upstream regulator involved in the promotion of enhanced proliferation, inflammation and fibrosis progression in Oct3$^{-/-}$ mice, as recently published (5,18). Also, gene expression analyses revealed that the majority of genes regulated by Hnf4α are activated in untraded Oct3$^{-/-}$ mice. But these data represent a pilot study and have to be evaluated critically. To further study the effect of loss of OCT function on HNF4α, Hnf4α mRNA expression was induced in stably OCT1- and OCT3-transfected tumour cell lines (HepG2 and HuH7) and primary Oct3$^{-/-}$ and WT hepatocytes after treatment with the non-selective OCT inhibitor quinine (P<0.01), showing n upregulation of Hnf4α mRNA expression with the loss of Oct function (Fig. 2A and B). Due to the transactivation of the OCT1 gene by HNF4α (6), a feedback mechanism is possible, but not identified yet. Interestingly, immunofluorescence of primary murine hepatocytes showed that Hnf4α was not only increased with escalating quinine doses, but the Hnf4α distribution also differed between Oct3$^{-/-}$ (nuclear) and WT (cytosol) hepatocytes (Fig. 2C), indicating that not only transcriptional loss of Oct3 but also functional loss of Oct affect Hnf4α. The fact that not only transcriptional but also functional factors play a relevant role in OCT regulation is in line with a previous characterisation of OCT3 as a cellular mechanism underlying rapid, non-genomic glucocorticoid regulation of monoaminergic neurotransmission, physiology and behaviour (38). OCT expression is regulated by transcriptional as well as complex epigenetic (39,40) and metabolic (41,42) factors. There is not a distinct pathway to explain

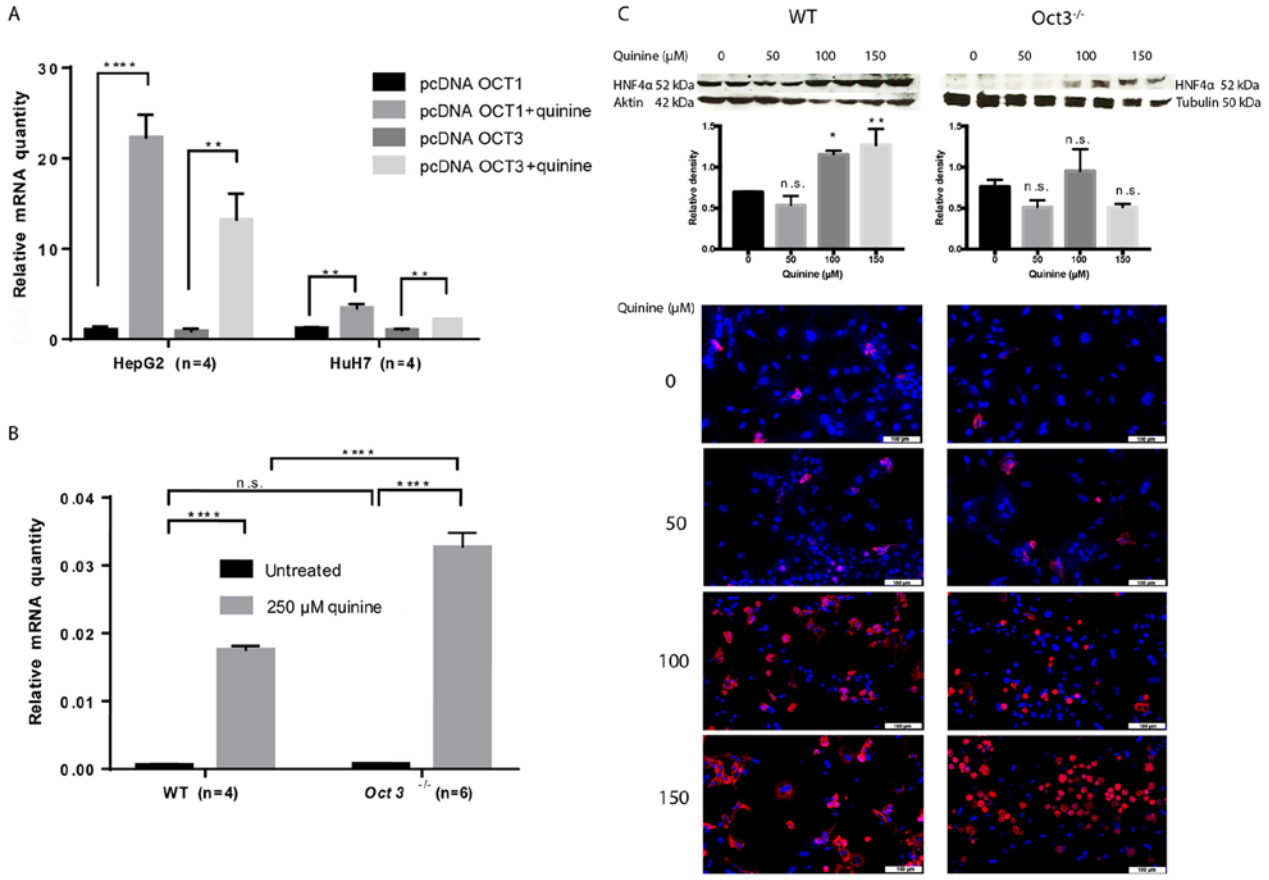

Figure 3. Oct inhibition leads to Hnf4α upregulation. (A) Hnf4α mRNA expression in stably OCT1 (pcDNAOCT1)- and OCT3 (pcDNAOCT3)-transfected HepG2 (n=4) and HuH7 (n=4) cells after 48 h of treatment with 250 μM of the non-selective OCT inhibitor quinine: OCT inhibition leads to Hnf4α mRNA upregulation. Values are expressed as fold expression relative to empty vector in transfected tumour cell lines. Control groups were HepG2 and HuH7 cells transfected with the empty vector. (B) Hnf4α mRNA expression in primary murine hepatocytes ($Oct3^{-/-}$): n=4, WT: n=6) after 48 h of treatment with 250 μM of the non-selective OCT inhibitor quinine: OCT inhibition leads to Hnf4α mRNA upregulation. Untreated primary murine hepatocytes served as control. (C) Representative western blots including densitometry and immunofluorescence (magnification, x10) in primary murine hepatocytes of two $Oct3^{-/-}$ and WT mice after 48 h treatment with escalating quinine doses (0, 50, 100 and 150 μM). *P<0.05; **P<0.01; ****P<0.0001 vs. 0 μM quinine. n.s., not significant; Hnf4α, hepatocyte nuclear factor 4α; $Oct3^{-/-}$, Oct3-knockout (FVB.Slc22a3tm10pb), WT, wild-type.

the function and mechanism of Oct3 in the context of liver damage. Therefore, the role of transcriptional and functional loss of Oct3 in Hnf4α regulation and finding a mechanistic link between Oct3 and Hnf4α needs further investigation.

For the first time, we show that Oct3 and Hnf4α regulation might be associated, with crucial effects on proliferation and fibrosis progression in the liver. Our results suggest that these transporters are key regulators of Hnf4α-dependent pathways. Further efforts are necessary to understand the complex regulation of Oct in the context of Hnf4α. Clinical relevance remains open. OCTs are emerged via gene duplication and substitute each other (39,40,43). Potentially a complete loss of Oct function is not compatible with life. This needs further studies

In conclusion, Hnf4α is downregulated in cholestasis and fibrosis and functional inhibition of OCT leads to the upregulation of Hnf4α. Thus, we present a novel link between the transporters and the Hnf4α network.

Acknowledgements

The authors would like to thank Mrs. Larissa Herbel (1st Department of Internal Medicine, Gastroenterology and Hepatology, University Medical Centre, Johannes Gutenberg-University Mainz, Mainz, Germany) and Mrs. Kim (Institute of Translational Immunology, Fibrosis and Metabolism Centre, Johannes Gutenberg-University Mainz, Mainz, Germany) for excellent technical support.

Funding

This work was supported by a MAIFOR grant from the Johannes Gutenberg University of Mainz to TZ. The funder only provided financial support.

Availability of data and materials

The sequencing datasets generated and/or analysed during the current study are available in the Gene Expression Omnibus repository under BioProject no. PRJNA685115 (http://www.ncbi.nlm.nih.gov/bioproject/685115). All other data are available on request.

Authors' contributions

JV and TZ designed research, performed experiments, collected and analysed data, and wrote the manuscript. JUM conducted

array data analysis. JV and TZ confirm the authenticity of all the raw data. PRG and DS made substantial contributions to interpretation of data. DS, JUM and PRG performed a critical review of the manuscript. YOK performed data analysis and provided methodological support. All authors read and approved the final manuscript.

Ethics approval and consent to participate

Animal care (housing, husbandry conditions) and animal procedures were performed in accordance with the European Council Directive of 24 November, 1986 (86/609/EEC). This study was approved by the state animal care commission (23 177-07/G 14-1-010). The study was not submitted to the institutional ethics committee/review board, but rather to the state animal care commission, because living mice and cell lines were used. No patient material was used.

Patient consent for publication

Not applicable.

Competing interests

The authors declare that they have no competing interests.

References

1. Heise M, Lautem A, Knapstein J, Schattenberg JM, Hoppe-Lotichius M, Foltys D, Weiler N, Zimmermann A, Schad A, Gründemann D, *et al*: Downregulation of organic cation transporters OCT1 (SLC22A1) and OCT3 (SLC22A3) in human hepatocellular carcinoma and their prognostic significance. BMC Cancer 12: 109, 2012.
2. Lautem A, Heise M, Gräsel A, Hoppe-Lotichius M, Weiler N, Foltys D, Knapstein J, Schattenberg JM, Schad A, Zimmermann A, *et al*: Downregulation of organic cation transporter 1 (SLC22A1) is associated with tumor progression and reduced patient survival in human cholangiocellular carcinoma. Int J Oncol 42: 1297-1304, 2013.
3. Grimm D, Lieb J, Weyer V, Vollmar J, Darstein F, Lautem A, Hoppe-Lotichius M, Koch S, Schad A, Schattenberg JM, *et al*: Organic Cation Transporter 1 (OCT1) mRNA expression in hepatocellular carcinoma as a biomarker for sorafenib treatment. BMC Cancer 16: 94, 2016.
4. Herraez E, Lozano E, Macias RI, Vaquero J, Bujanda L, Banales JM, Marin JJ and Briz O: Expression of SLC22A1 variants may affect the response of hepatocellular carcinoma and cholangiocarcinoma to sorafenib. Hepatology 58: 1065-1073, 2013.
5. Vollmar J, Lautem A, Closs E, Schuppan D, Kim YO, Grimm D, Marquardt JU, Fuchs P, Straub BK, Schad A, *et al*: Loss of organic cation transporter 3 (Oct3) leads to enhanced proliferation and hepatocarcinogenesis. Oncotarget 8: 115667-115680, 2017.
6. Saborowski M, Kullak-Ublick GA and Eloranta JJ: The human organic cation transporter-1 gene is transactivated by hepatocyte nuclear factor-4alpha. J Pharmacol Exp Ther 317: 778-785, 2006.
7. Rulcova A, Krausova L, Smutny T, Vrzal R, Dvorak Z, Jover R and Pavek P: Glucocorticoid receptor regulates organic cation transporter 1 (OCT1, SLC22A1) expression via HNF4alpha upregulation in primary human hepatocytes. Pharmacol Rep 65: 1322-1335, 2013.
8. Parviz F, Matullo C, Garrison WD, Savatski L, Adamson JW, Ning G, Kaestner KH, Rossi JM, Zaret KS and Duncan SA: Hepatocyte nuclear factor 4alpha controls the development of a hepatic epithelium and liver morphogenesis. Nat Genet 34: 292-296, 2003.
9. Sasaki S, Urabe M, Maeda T, Suzuki J, Irie R, Suzuki M, Tomaru Y, Sakaguchi M, Gonzalez FJ and Inoue Y: Induction of hepatic metabolic functions by a novel variant of hepatocyte nuclear factor 4γ. Mol Cell Biol 8: e00213-18, 2018.
10. Ning BF, Ding J, Yin C, Zhong W, Wu K, Zeng X, Yang W, Chen YX, Zhang JP, Zhang X, *et al*: Hepatocyte nuclear factor 4 alpha suppresses the development of hepatocellular carcinoma. Cancer Res 70: 7640-7651, 2010.
11. Walesky C, Edwards G, Borude P, Gunewardena S, O'Neil M, Yoo B and Apte U: Hepatocyte nuclear factor 4 alpha deletion promotes diethylnitrosamine-induced hepatocellular carcinoma in rodents. Hepatology 57: 2480-2490, 2013.
12. Saha SK, Parachoniak CA, Ghanta KS, Fitamant J, Ross KN, Najem MS, Gurumurthy S, Akbay EA, Sia D, Cornella H, *et al*: Mutant IDH inhibits HNF-4alpha to block hepatocyte differentiation and promote biliary cancer. Nature 513: 110-114, 2014.
13. Wu N, Zhang YL, Wang HT, Li DW, Dai HJ, Zhang QQ, Zhang J, Ma Y, Xia Q, Bian JM and Hang HL: Overexpression of hepatocyte nuclear factor 4α in human mesenchymal stem cells suppresses hepatocellular carcinoma development through Wnt/β-catenin signaling pathway downregulation. Cancer Biol Ther 17: 558-565, 2016.
14. Yue HY, Yin C, Hou JL, Zeng X, Chen YX, Zhong W, Hu PF, Deng X, Tan YX, Zhang JP, *et al*: Hepatocyte nuclear factor 4alpha attenuates hepatic fibrosis in rats. Gut 59: 236-246, 2010.
15. Fan TT, Hu PF, Wang J, Wei J, Zhang Q, Ning BF, Yin C, Zhang X, Xie WF, Chen YX and Shi B: Regression effect of hepatocyte nuclear factor 4alpha on liver cirrhosis in rats. J Dig Dis 14: 318-327, 2013.
16. Park MR, Wong MS, Araúzo-Bravo MJ, Lee H, Nam D, Park SY, Seo HD, Lee SM, Zeilhofer HF, Zaehres H, *et al*: Oct4 and Hnf4α-induced hepatic stem cells ameliorate chronic liver injury in liver fibrosis model. PLoS One 14: e0221085, 2019.
17. Zwart R, Verhaagh S, Buitelaar M, Popp-Snijders C and Barlow DP: Impaired activity of the extraneuronal monoamine transporter system known as uptake-2 in Orct3/Slc22a3-deficient mice. Mol Cell Biol 21: 4188-4196, 2001.
18. Vollmar J, Kim YO, Marquardt JU, Becker D, Galle PR, Schuppan D and Zimmermann T: Deletion of organic cation transporter Oct3 promotes hepatic fibrosis via upregulation of TGFβ. Am J Physiol Gastrointest Liver Physiol 317: G195-G202, 2019.
19. Jonker JW and Schinkel AH: Pharmacological and physiological functions of the polyspecific organic cation transporters: OCT1, 2, and 3 (SLC22A1-3). J Pharmacol Exp Ther 308: 2-9, 2004.
20. Jonker JW, Wagenaar E, Van Eijl S and Schinkel AH: Deficiency in the organic cation transporters 1 and 2 (Oct1/Oct2 [Slc22a1/Slc22a2]) in mice abolishes renal secretion of organic cations. Mol Cell Biol 23: 7902-7908, 2003.
21. Moll P, Ante M, Seitz A and Reda T: QuantSeq 3'mRNA sequencing for RNA quantification. Nat Methods 12, 2014.
22. Liao Y, Smyth GK and Shi W: The Subread aligner: Fast, accurate and scalable read mapping by seed-and-vote. Nucleic Acids Res 41: e108, 2013.
23. Morgan M, Anders S, Lawrence M, Aboyoun P, Pagès H and Gentleman R: ShortRead: A bioconductor package for input, quality assessment and exploration of high-throughput sequence data. Bioinformatics 25: 2607-2608, 2009.
24. Love MI, Huber W and Anders S: Moderated estimation of fold change and dispersion for RNA-seq data with DESeq2. Genome Biol 15: 550, 2014.
25. Kim YO, Popov Y and Schuppan D: Optimized mouse models for liver fibrosis. Methods Mol Biol 1559: 279-296, 2017.
26. Nies AT, Koepsell H, Winter S, Burk O, Klein K, Kerb R, Zanger UM, Keppler D, Schwab M and Schaeffeler E: Expression of organic cation transporters OCT1 (SLC22A1) and OCT3 (SLC22A3) is affected by genetic factors and cholestasis in human liver. Hepatology 50: 1227-1240, 2009.
27. Denk GU, Soroka CJ, Mennone A, Koepsell H, Beuers U and Boyer JL: Down-regulation of the organic cation transporter 1 of rat liver in obstructive cholestasis. Hepatology 39: 1382-1389, 2004.
28. Tag CG, Sauer-Lehnen S, Weiskirchen S, Borkham-Kamphorst E, Tolba RH, Tacke F and Weiskirchen R: Bile duct ligation in mice: induction of inflammatory liver injury and fibrosis by obstructive cholestasis. J Vis Exp: 52438, 2015.
29. Li WC, Ralphs KL and Tosh D: Isolation and culture of adult mouse hepatocytes. Methods Mol Biol 633: 185-196, 2010.
30. Arndt P, Volk C, Gorboulev V, Budiman T, Popp C, Ulzheimer-Teuber I, Akhoundova A, Koppatz S, Bamberg E, Nagel G and Koepsell H: Interaction of cations, anions, and weak base quinine with rat renal cation transporter rOCT2 compared with rOCT1. Am J Physiol Renal Physiol 281: F454-F468, 2001.

31. Müller J, Lips KS, Metzner L, Neubert RH, Koepsell H and Brandsch M: Drug specificity and intestinal membrane localization of human organic cation transporters (OCT). Biochem Pharmacol 70: 1851-1860, 2005.
32. Koepsell H: Polyspecific organic cation transporters: Their functions and interactions with drugs. Trends Pharmacol Sci 25: 375-381, 2004.
33. Koepsell H, Lips K and Volk C: Polyspecific organic cation transporters: structure, function, physiological roles, and biopharmaceutical implications. Pharm Res 24: 1227-1251, 2007.
34. Keller T, Elfeber M, Gorboulev V, Reiländer H and Koepsell H: Purification and functional reconstitution of the rat organic cation transporter OCT1. Biochemistry 44: 12253-12263, 2005.
35. van der Velden M, Bilos A, van den Heuvel JJMW, Rijpma SR, Hurkmans EGE, Sauerwein RW, Russel FGM and Koenderink JB: Proguanil and cycloguanil are organic cation transporter and multidrug and toxin extrusion substrates. Malar J 16: 422, 2017.
36. Hilgendorf C, Ahlin G, Seithel A, Artursson P, Ungell AL and Karlsson J: Expression of thirty-six drug transporter genes in human intestine, liver, kidney, and organotypic cell lines. Drug Metab Dispos 35: 1333-1340, 2007.
37. Hagos Y, Wegner W, Kuehne A, Floerl S, Marada VV, Burckhardt G and Henjakovic M: HNF4α induced chemosensitivity to oxaliplatin and 5-FU mediated by OCT1 and CNT3 in renal cell carcinoma. J Pharm Sci 103: 3326-3334, 2014.
38. Gasser PJ and Lowry CA: Organic cation transporter 3: A cellular mechanism underlying rapid, non-genomic glucocorticoid regulation of monoaminergic neurotransmission, physiology, and behavior. Horm Behav 104: 173-182, 2018.
39. Sleutels F, Tjon G, Ludwig T and Barlow DP: Imprinted silencing of Slc22a2 and Slc22a3 does not need transcriptional overlap between Igf2r and Air. EMBO J 22: 3696-3704, 2003.
40. Sleutels F, Zwart R and Barlow DP: The non-coding Air RNA is required for silencing autosomal imprinted genes. Nature 415: 810-813, 2002.
41. Chen L, Shu Y, Liang X, Chen EC, Yee SW, Zur AA, Li S, Xu L, Keshari KR, Lin MJ, *et al*: OCT1 is a high-capacity thiamine transporter that regulates hepatic steatosis and is a target of metformin. Proc Natl Acad Sci USA 111: 9983-9988, 2014.
42. Chen L, Hong C, Chen EC, Yee SW, Xu L, Almof EU, Wen C, Fujii K, Johns SJ, Stryke D, *et al*: Genetic and epigenetic regulation of the organic cation transporter 3, SLC22A3. Pharmacogenomics J 13: 110-120, 2013.
43. Nagano T, Mitchell JA, Sanz LA, Pauler FM, Ferguson-Smith AC, Feil R and Fraser P: The Air noncoding RNA epigenetically silences transcription by targeting G9a to chromatin. Science 322: 1717-1720, 2008.